Opportunistic Scheduling for Single-downlink Satellite-based Quantum Key Distribution

MD ZAKIR HOSSAIN, University of Connecticut, USA
NITISH K. PANIGRAHY, Binghamton University, USA
WALTER O. KRAWEC, University of Connecticut, USA
DON TOWSLEY, University of Massachusetts Amherst, USA
BING WANG*, University of Connecticut, USA

Satellite-based quantum key distribution (QKD), leveraging low photon loss in free-space quantum communication, is widely regarded as one of the most promising directions to achieve global-scale QKD. With a constellation of satellites and a set of ground stations in a satellite-based QKD system, how to schedule satellites to achieve efficient QKD is an important problem. This problem has been studied in the dual-downlink architecture, where each satellite distributes pairs of entanglements to two ground stations simultaneously. However, it has not been studied in the single downlink architecture, where satellites create keys with each individual ground station, and then serve as trusted nodes to create keys between pairs of ground stations. While the single downlink architecture provides weaker security in that the satellites need to be trusted, it has many advantages, including the potential of achieving significantly higher key rates, and generating keys between pairs of ground stations that are far away from each other and cannot be served using the dual-downlink architecture. In this paper, we propose a novel opportunistic approach for satellite scheduling that accounts for fairness among the ground station pairs, while taking advantage of the dynamic satellite channels to maximize the system performance. We evaluate this approach in a wide range of settings and demonstrate that it provides the best tradeoffs in terms of total and minimum key rates across the ground station pairs. Our evaluation also highlights the importance of considering seasonal effects and cloud coverage in evaluating satellite-based QKD systems. In addition, we show different tradeoffs in global and regional QKD systems.

1 Introduction

Satellite-based quantum key distribution (QKD) allows two ground stations A and B that are far away from each other to establish shared secret keys using QKD protocols that provide information-theoretic security [30]. It is widely regarded as one of the most promising directions to achieve global-scale QKD, since free-space quantum communication between satellites and ground stations leads to much lower photon loss compared to photon communication on the ground [6–8, 16, 21, 34]. The feasibility of satellite-based QKD has been demonstrated experimentally [22, 37, 38, 42]. On the other hand, many challenges remain to make satellite-based QKD into an efficient and commercially-viable system.

Consider a satellite-based QKD system with a constellation of satellites and a set of ground stations. The quantum communication can be *downlink*, from satellites to ground stations, or *uplink*, from ground stations to satellites. The downlink direction has an advantage over the uplink direction due to lower photon loss in the initial stage [8]. In this paper, we focus on a *single-downlink* architecture, where a satellite sends photons to ground stations individually, and then serves as a common node to establish shared keys between two ground stations. This differs from a dual-downlink architecture, where a satellite sends entangled pairs to two ground stations *simultaneously*

Authors' Contact Information: Md Zakir Hossain, University of Connecticut, Storrs, Connecticut, USA; Nitish K. Panigrahy, Binghamton University, Binghamton, New York, USA; Walter O. Krawec, University of Connecticut, Storrs, Connecticut, USA; Don Towsley, University of Massachusetts Amherst, Amherst, Massachusetts, USA; Bing Wang, University of Connecticut, Storrs, Connecticut, USA.

to establish a shared secret key directly between them. While single-downlink architecture requires that satellites need to be trusted (since they serve as trusted nodes), and hence has weaker security than the dual-downlink architecture where the satellites do not need to be trusted, it has several other advantages in terms of cost, efficiency and coverage. First, the single-downlink architecture only requires satellites to generate photons, instead of entanglements, and hence are simpler and less costly than the dual-downlink architecture. Secondly, since the single-downlink architecture involves quantum communication along one link, i.e., between a satellite and a ground station, instead of along two links, between a satellite and two ground station simultaneously, it has a higher success rate per round, and hence can produce a higher key rate than the dual-downlink architecture. Last, the single-downlink architecture does not require a satellite to be in view of two ground stations simultaneously, hence it can achieve key establishment among ground stations that are much farther apart than what is feasible with dual-downlink settings. As an example, in a prior study [26], no key could be established between New York City and Houston in the U.S. when using satellites at altitude of 500 km (polar constellation) in the dual-downlink setting, while it can be easily achieved in the single-donwlink setting (see §6).

Since a ground station can be served by multiple satellites in the single-downlink architecture at one point of time, satellite scheduling determines which satellites serve which ground stations. A scheduling algorithm needs to satisfy the constraints of the satellites and ground stations. It also needs to be efficient, maximizing system performance, while being fair to the ground stations. While satellite scheduling has been studied in the dual-downlink setting [11, 26, 28, 39, 40], scheduling in the single downlink architecture for key establishment among ground station pairs has not received much attention (see §7). In this paper, we formulate the problem and develop efficient solutions that consider both system performance and fairness among the ground station pairs.

Our work makes the following contributions:

• We formulate the satellite scheduling problem for the single-downlink setting for QKD systems and develop two comparison baselines that optimize minimum and total key sizes across the ground station pairs, respectively (§3).

• We develop an opportunistic scheduling framework where schedulers take advantage of the dynamic and diverse satellite to ground station channels for efficient key establishment among ground station pairs (§4). Our approach works in two phases. Phase 1 extends opportunistic scheduling approaches [24, 25] in classical wireless communication to multi-satellite settings for key establishment between satellites and ground stations (§5). Phase 2 uses an iterative optimization approach to establish keys for ground station pairs assisted by the satellites. This two-phase approach can balance fairness and total key size, and has significantly lower computation overhead than the two baseline schemes.

• Using extensive simulation in a wide range of settings, we demonstrate that our opportunistic scheduling framework achieves the best tradeoffs in terms of total and minimum key rates across the ground station pairs among all the schemes we evaluate (§6). Our evaluation further highlights the importance of considering seasonal effects and cloud coverage in evaluating satellite-based QKD systems. In addition, we show different tradeoffs in global and regional QKD systems.

2 Background

2.1 Single-downlink Satellite-assisted QKD

We consider a constellation of satellites in low-earth orbit (LEO) that facilitate QKD for a set of ground stations on Earth; see Fig. 1. In the rest of the paper, we assume that the satellites follow a Polar constellation; our approach is applicable to other types of constellations (e.g., Walker, Iridium,
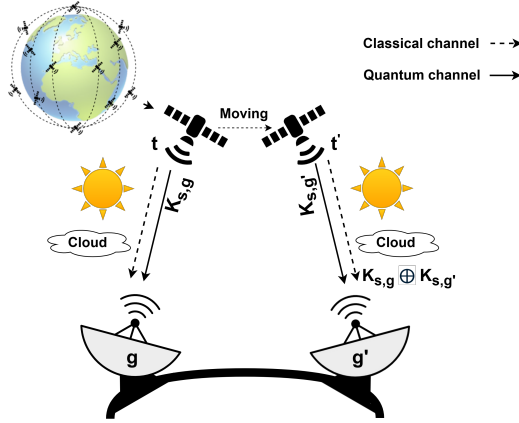
Fig. 1. Single-downlink satellite-assisted QKD system. A satellite runs a QKD protocol with individual ground stations, and then uses classical channels and one-time pad to establish secret keys for ground station pairs.

Starlink, and Kuiper [21]). Similarly, our approach is not limited to LEO satellites; we focus on LEO satellites due to their proximity to the Earth, which can lead to high key rates.

In the single-downlink setting, a satellite establishes secret keys with each ground station individually using a prepare-and-measure QKD protocol, e.g., BB84 [9]. Specifically, each satellite is equipped with a photon generation source. When a satellite is in view of a ground station, it generates quantum states and sends them to the ground station through a free-space optical channel. The ground station measures the received photons using randomly chosen bases, resulting in correlated raw key bits between the two parties.

We next briefly describe the BB84 QKD protocol, which we use in the rest of the paper. For a general QKD survey, see [31]. QKD protocols operate in two stages: a quantum communication stage, followed by a classical post processing stage. During the former, photons (which can encode quantum bits through polarization encoding [31]) are transmitted from the satellite, which attempts to encode secret key material onto the photon by encoding the classical data using one of two mutually unbiased bases (MUBs), chosen randomly. Two bases are mutually unbiased if the magnitude squared of the inner product of any vector from one, with any vector from another, is $1/d$, with d being the dimension of the system; $d = 2$ in the qubit case. These photons/qubits travel to the ground station where they are subsequently measured, with the measurement being performed in one of two MUBs. If the satellite and the ground station select the same basis, then the satellite and ground station should have a correlated bit; otherwise, the round is discarded. Over many rounds, the satellite and the ground station obtain correlated bits and pool them into a *raw key*. These raw keys (one held by the satellite and one by the ground station) are partially correlated, as noise may have caused some measurement error, and partially secret, an adversary may have some partial information on the raw key. Thus, they cannot be used directly as secret keys and must be further processed through additional classical processing in the second stage.

The post-processing phase utilizes a classical authenticated channel, and consists of two steps. First, an error-correction protocol is applied to reconcile discrepancies caused by channel losses, background photons, and detector imperfections. Second, privacy amplification is performed which takes in the, now error corrected, raw key and outputs a new, smaller, secret key. This is done by mapping the raw key through a two-universal hash function. The outcome is a shorter, but secure, secret key shared between the satellite and the ground station which is subsequently added to a

key-pool for these users (i.e., a secret bit string, held by both parties, that is both secret and fully correlated). Note that this key-pool may also be considered a single, large, secret key.

An important question is: given the observed noise level in the raw key, how large will the final secret key be, after privacy amplification is run? Let N denote the number of raw key rounds exchanged between satellite s and ground station g. After error correction and privacy amplification, let ℓ denote the size of the final secret key (after privacy amplification). The *secret key rate* is, then, defined as $r = \ell/N$.

In the asymptotic regime, where $N \to \infty$, the secret key rate can be expressed as [33]

$$r = 1 - 2h(E), \tag{1}$$

where E is the error rate of the raw key, and $h(x) = -x \log x - (1-x) \log(1-x)$ is the binary entropy function. Note that, in practice, E can be estimated through classical sampling methods, by having the satellite and ground station disclose a random portion of their produced raw key, and subsequently discarding the sampled portion of the key.

Of course, the above is for one satellite and one ground station. However, the goal is to allow two ground stations to establish a shared secret key. For this, the satellite will be used as a trusted node in the following manner. Let $K_{s,g}$ represent the set of key bits established between satellite s and ground station g after a sufficient number of rounds of QKD (i.e., $K_{s,g}$ is the key-pool for this particular satellite and ground station pair). Similarly, let $K_{s,g'}$, represent the key-pool shared between satellite s and a different ground station g'. Then, through classical communication channels, satellite s sends $K_{s,g} \oplus K_{s,g'}$ to g'. This allows g' to learn $K_{s,g}$ by performing the operation $K_{s,g} \oplus K_{s,g'} \oplus K_{s,g'}$. At this point, $K_{s,g}$ is now a shared secret key between ground station g and g'.

In the above process, the secret key pool $K_{s,g'}$, shared, initially, between s and g', was used as a secret key to encrypt $K_{s,g}$ via the one-time pad encryption algorithm, which is a perfectly secret method of encryption [19]. However, OTP requires that a secret key be used only once and that the key be as large as the message being encrypted. This puts two constraints on the above process: First, once $K_{s,g'}$ is used to allow g and g' to share a key (namely, to share $K_{s,g}$), then it cannot be used again and must be discarded. Second, $K_{s,g'}$ must be as large as, or larger than, $K_{s,g}$. If it is shorter, then only $|K_{s,g'}|$ bits may be encrypted. Thus, ultimately, g and g' will have a secret key of size $\min(|K_{s,g}|, |K_{s,g'}|)$; the rest of the key pool can be used later.

2.2 Loss and Noise Models

The free-space optical (FSO) channel between a satellite and a ground station introduces loss and noise that strongly influence the performance of quantum key distribution. Transmission loss increases quadratically with propagation distance and is further affected by the elevation angle[1] and atmospheric conditions [26].

Consider a satellite s and ground station g. At time t, let the elevation angle be $\theta_{s,g}(t)$ and the line-of-sight distance between the satellite and ground station be $D_{s,g}(t)$. Let $\alpha_g(t)$ denote atmospheric profile above ground station g at time t. This profile captures time-varying environmental parameters, including temperature, pressure and humidity, that affect photon attenuation in the atmosphere. In particular, for each ground station, we consider four representative atmospheric profiles corresponding to the solstices and equinoxes (see later). We model the optical channel as a Bosonic pure-loss channel with time-varying transmissivity $\eta_{s,g}(t)$, which attenuates the transmitted quantum state and reduces the probability of successful photon detection. We compute

---

[1]The elevation angle, $\theta_{s,g}(t)$, is defined as the angle between the horizontal plane at g and the line-of-sight from g to the satellite s.

the end-to-end transmissivity as:

$$\eta_{s,g}(t) = \underbrace{\eta_{\text{fs}}(D_{s,g}(t))}_{\text{free-space}} \cdot \underbrace{\eta_{\text{atm}}(\alpha_g(t), \theta_{s,g}(t))}_{\text{atmosphere}} \cdot \underbrace{\eta_{opt}}_{\text{optics}} . \tag{2}$$

Here, η_{opt} captures coupling and other internal losses at the source and receiver hardware. The free space transmissivity η_{fs} captures photon losses due to diffraction and decays quadratically as a function of $D_{s,g}(t)$. The atmospheric transmissivity η_{atm} accounts for photon losses due to absorption and scattering in the atmosphere and is expressed as [13]:

$$\eta_{\text{atm}}(\alpha_g(t), \theta_{s,g}(t)) = [\hat{\eta}_{\text{atm}}(\alpha_g(t))]^{\text{cosec}(\theta_{s,g}(t))}, \tag{3}$$

where $\hat{\eta}_{\text{atm}}$ is the atmospheric transmissivity at zenith. Seasonal variation is incorporated by generating atmospheric profiles for representative days in March, June, September, and December at each ground station location, which are used in our evaluation in §6. To compute $\hat{\eta}_{\text{atm}}$ for a given atmospheric profile $\alpha_g(t)$, we use MODTRAN (Moderate Spectral Resolution Radiative Transfer Model) software [2] under clear-sky conditions with complete visibility and zero cloud cover.

Clouds introduce losses or in some cases complete blockage of satellite-to-ground optical links. To model this effect, we incorporate time and location dependent cloud coverage data, denoted by a cloud factor $c_{t,g} \in [0, 1]$, where $c_{t,g} = 0$ corresponds to clear sky and $c_{t,g} = 1$ represents full obstruction of the downlink at ground station g at time t. We obtain these cloud coverage data at an hourly scale from the Visual Crossing Weather API [3].

In addition to transmission losses, quantum states encoded in photons are impaired by background photons and detector dark counts. During daylight hours, these background photons primarily originate from ambient solar radiation and contributes to unwanted detection events at the ground station. The background photon count is highly time-dependent: during daylight hours, especially near noon, solar radiation induces elevated noise levels, whereas at night, the background photon flux is substantially lower. We evaluate this variation by sampling background photon flux at four representative times: 12:00 AM, 6:00 AM, 12:00 PM and 6:00 PM, for each ground station location. We model the arrival of background photons at the ground station telescope as spurious detection events that increase the quantum bit error rate. Finally, detector dark counts are included as a constant probability of false clicks per detection window. Together, these effects determine the overall signal photon detection probability, the quantum bit error rate, and ultimately the achievable secret key rate in single-downlink QKD.

3 Problem Setting and Comparison Baselines

In this section, we first present the problem setting, and then two optimization-based formulations that will be used as comparison baselines to evaluate our proposed opportunistic solutions.

3.1 Problem Setting

Let $\mathcal{S}$ denote a set of satellites and $\mathcal{G}$ denote a set of ground stations. Consider a time interval (e.g., a day). Time is divided into discrete slots (e.g., each slot is one second) indexed by $t \in \{1, 2, \dots, T\}$. During each slot, a satellite $s \in \mathcal{S}$ may run QKD with a ground station $g \in \mathcal{G}$ using the downlink quantum channel, provided that the satellite is above the horizon of the ground station and satisfies a minimum elevation angle requirement θ.

At any point of time, a satellite can be in view of multiple ground stations. Similarly, a ground station can be in view of multiple satellites. Let $M_s \geq 1$ denote the number of transmitters at satellite s and $R_g \geq 1$ denote the number of receivers at ground station g. In other words, in each slot, satellite s can serve up to M_s ground stations, while ground station g can be served by up to R_g satellites. The scheduling problem is to determine, for any slot t, a subset of satellites (no more

than R_g) in $\mathcal{S}$ that will serve each ground station, $g \in \mathcal{G}$ so that the constraints of each satellite and ground station are satisfied. The goal is to achieve a high aggregate key rate across all satellite ground station assignments while providing a fair allocation of resources among ground station pairs.

For slot t, let $\lambda_t^{s,g}$ denote the number of photons that satellite s distributes to ground station g successfully in the slot, and let $\mathsf{R}_t^{s,g}$ denote the corresponding key-rate. Prior to computing a schedule, we first estimate $\lambda_t^{s,g}$ using the loss model in §2.2. Similarly, we estimate $\mathsf{R}_t^{s,g}$ by accounting for errors using the noise model in §2.2 and key rate expression (1).

Let $c_{t,g}$ denote the cloud coverage for ground station g in slot t, which is also estimated ahead of time based on weather prediction as described in §2.2. Therefore, for slot t, following the linear approximation in [32], the number of secret keys generated by satellite s serving ground station g is $(1 - c_{t,g})\lambda_t^{s,g}\mathsf{R}_t^{s,g}$. In the rest of the paper, for ease of exposition, let $n_t^{s,g} := (1 - c_{t,g})\lambda_t^{s,g}\mathsf{R}_t^{s,g}$ denote the number of secret keys that can be generated in slot t between satellite s and ground station g.

Following a scheduling algorithm, let $K_{s,g}$ represent the set of key bits that satellite s has established with ground station g at the end of time T. Since the goal is establishing shared keys among ground station pairs, satellite s needs to further determine what fraction of the key bits in $K_{s,g}$ is used to create shared keys with another ground station, g'. Let $\mathcal{U} = \{u \mid u = (g, g'), g' > g\}$ denote the set of ground station pairs where, for each ground station pair $u = (g, g')$, we represent the ground stations in increasing order of their indices. Let $y_{s,u}$ represent the number of key bits that are established for ground station pair u through satellite s. Since the shared key bits for u via s are obtained by XOR'ing the key bits in $K_{s,g}$ with those in $K_{s,g'}$, we need $|K_{s,g}| \geq y_{s,u}$, and $|K_{s,g'}| \geq y_{s,u}$, where $|K_{s,g}|$ represents the number of key bits in $K_{s,g}$. The size of the key that is established for ground station pair u considering all the satellites is therefore $\sum_s y_{s,u}$.

One goal of satellite scheduling is to achieve maxmin optimization, i.e., maximizing the minimum key size across all the ground station pairs. However, since some ground stations may be in unfavorable conditions (e.g., due to its position or adverse weather conditions), such a scheduling objective may result in a reduced total key size across all ground station pairs. Another optimization goal is to maximize the total key size, which, however, may cause some ground station pairs to have small key sizes. Therefore, a good goal is balancing both fairness and total key size.

3.2   Comparison Baselines

We next present two optimization formulations for satellite scheduling, *Max-Min* and *Max-Sum*. Max-Min aims to maximize the minimum of $\sum_s y_{s,u}$. Max-Sum aims to maximize $\sum_s \sum_u y_{s,u}$, i.e., the total key size across all the ground station pairs through all the satellites. Let K_{maxmin} and K_{maxsum} denote respectively the objective values from these two optimization problems. Then a good scheduling algorithm should have the minimum key size across all the ground station pairs close to K_{maxmin} and the total key size across all the ground station pairs close to K_{maxsum}. In the rest of the paper, we use these two quantities to evaluate satellite scheduling algorithms.

Consider slot t. Let $x_t^{s,g}$ denote a binary decision variable; $x_t^{s,g} = 1$ if satellite s serves ground station g in slot t, and $x_t^{s,g} = 0$ otherwise. Another decision variable is integer variable, $y_{s,u}$, which represents the size of the key established for ground station pair u through satellite s. The two optimization problems consider all the slots in $\{1, \ldots, T\}$ as follows

$$\text{Max-Min:} \quad \text{maximize:} \quad \min_u \sum_{s \in \mathcal{S}} y_{s,u} \tag{4}$$

$$\text{Max-Sum:} \quad \text{maximize:} \quad \sum_{u \in \mathcal{U}} \sum_{s \in \mathcal{S}} y_{s,u} \tag{5}$$

$$\text{s.t.} \sum_{g \in \mathcal{G}} x_t^{s,g} \leq M_s, \qquad \forall s \in \mathcal{S}, t = 1, \dots, T \tag{6}$$

$$\sum_{s \in \mathcal{S}} x_t^{s,g} \leq R_g, \qquad \forall g \in \mathcal{G}, t = 1, \dots, T \tag{7}$$

$$\sum_{t=1}^{T} n_t^{s,g} x_t^{s,g} \geq \sum_{\forall u \text{ s.t. } g \in u} y_{s,u}, \qquad \forall s \in \mathcal{S}, \forall g \in \mathcal{G} \tag{8}$$

$$x_t^{s,g} \in \{0, 1\}, \qquad \forall s \in \mathcal{S}, \forall g \in \mathcal{G}, t = 1, \dots, T \tag{9}$$

$$y_{s,u} \in Z, \qquad \forall s \in \mathcal{S}, \forall u \in \mathcal{U} \tag{10}$$

In the above, (4) and (5) are the objective functions for Max-Min and Max-Sum optimization, respectively. Eq. (6) represents the constraint on the number of transmitters for each satellite, while (7) represents the constraint on the number of receivers for each ground station. Eq. (8) indicates that the total number of key bits that satellite s generates for ground station g needs to be no less than the number of key bits that is used to generate pairwise keys for all the pairs that include g. Last, (9) and (10) specify that $x_t^{s,g}$ and $y_{s,u}$ are binary and integer variables, respectively.

The above optimization problems are mixed-integer programming (MIP) problems, which can be solved using standard MIP solvers (e.g., CPLEX [1]). The total number of decision variables is $T|\mathcal{G}||\mathcal{S}| + |\mathcal{S}||\mathcal{U}|$. Even though we can remove some of the decision variables, e.g., $x_t^{s,g}$ if satellite s is not in view of ground station g in slot t, the number of decision variables can still be very large for a large number of satellites and ground stations. In §4, we propose a more efficient opportunistic scheduling framework.

4 Opportunistic Scheduling Framework

Our proposed opportunistic scheduling framework divides the problem into two phases; see Fig. 2. Phase 1 assigns satellite to ground stations to determine $K_{s,g}$, $\forall s \in \mathcal{S}$ and $g \in \mathcal{G}$ at the end of time T, and Phase 2 further determines pairwise keys for each ground station pair through each satellite, i.e., $y_{s,u}$ given $K_{s,g}$, $\forall s \in \mathcal{S}$, $g \in \mathcal{G}$, and $u \in \mathcal{U}$. These two phases are closely related: to achieve efficient and fair key establishment in Phase 2, the satellite assignment in Phase 1 needs to be efficient and fair. Consider an extreme case. Suppose that satellite s generates a large number of key bits with only one ground station. Then all these key bits are useless in Phase 2, since satellite s also needs to have key bits with other ground stations to be able to perform XOR operations to establish keys between g and other ground stations. Therefore, in Phase 1, a natural goal is to achieve fair scheduling so that each satellite s generate similar numbers of key bits across the ground stations.

• **Phase 1:** Opportunistic scheduling for QKD between satellites and ground stations. Consider a satellite, s. The number of key bits that s generates with the ground stations can vary significantly due to multiple factors such as the locations and dynamics in transmissivity and weather conditions. Scheduling the satellite to serve the ground stations over time is akin to scheduling a base station to serve multiple users in wireless communication (e.g., cellular network systems), which has been extensively studied. We leverage *opportunistic scheduling*, a well-established framework in the area of wireless communication (see survey [5] and the references within), to solve this problem. The
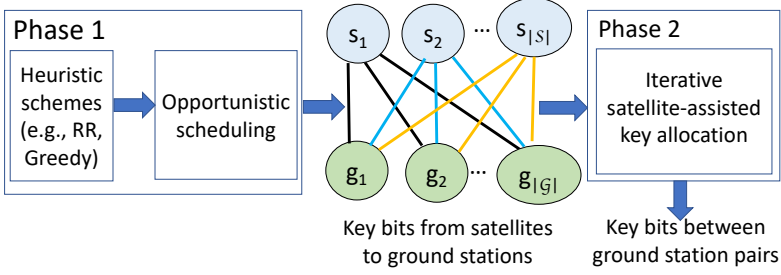
Fig. 2. Opportunistic scheduling framework. Phase 1 schedules satellites to establish keys with individual ground stations, leading to key bits, $K_{s,g}$ between satellite s and ground station g, $\forall s, \forall g$, colored in the figure based on the satellites. Phase 2 uses iterative optimization to establish keys among the ground station pairs.

main idea of opportunistic scheduling is to dynamically assign transmission resources, e.g., time slots, subcarriers, or power, to users based on their instantaneous channel conditions. It exploits the natural variability in wireless channels across multiple users (e.g., due to fading, multipath, and mobility) to opportunistically serve users with favorable channel conditions to maximize overall system performance, while potentially balancing trade-offs in QoS (e.g., delay, jitter) and fairness.

The satellite scheduling problem in our setting, however, differs from the typical setup in that we need to schedule multiple satellites to serve a set of ground stations with constraints on the number of transmitters for the satellites and number of receivers for the ground stations. In addition, for one satellite, it is only in view of a subset of ground stations, or no ground station at all, for a large number of slots. We describe our opportunistic satellite scheduling algorithm in §5.

• **Phase 2:** Satellite-assisted key assignments to ground station pairs. The second phase can be easily solved through a maxmin formulation with the decision variables $y_{s,u}$, $\forall s \in \mathcal{S}, u \in \mathcal{U}$, taking $K_{s,g}$, $\forall s \in \mathcal{S}, g \in \mathcal{G}$ obtained by Phase 1 as the input.

$$\text{maximize:} \quad \min_{u} \sum_{s} y_{s,u} \tag{11}$$

$$\text{s.t.} \quad \sum_{\forall u \text{ s.t. } g \in u} y_{s,u} \le |K_{s,g}|, \qquad \forall s \in \mathcal{S}, \forall g \in \mathcal{G} \tag{12}$$

$$y_{s,u} \in Z, \qquad \forall s \in \mathcal{S}, \forall u \in \mathcal{U} \tag{13}$$

The above problem is also an MIP problem and can be solved using standard MIP solvers. It has $|\mathcal{S}||\mathcal{U}|$ decision variables and hence is much easier to solve than the formulation in (4). We solve the above problem iteratively. That is, after the first iteration, we remove the key bits that have been allocated, and the ground station pairs that have key bits equal to the obtained objective function value (i.e., no more keys can be established for them) so that they are not considered in the next round. The process continues until no more keys can be established between any ground station pair.

5 Phase 1 Opportunistic Scheduling

In this section, we detail our design of opportunistic satellite scheduling, i.e., the problem in Phase 1 in our proposed framework (see §4). For ease of exposition, we first consider the case of a single satellite serving a set of ground stations, and then extend the solution to a constellation of multiple satellites. Unless otherwise specified, we consider the realistic scenario where each ground station has a single receiver, i.e., $R_g = 1$, and each satellite has a single transmitter, i.e., $M_s = 1$; our approach can be easily extended to the more general case of multiple receivers and transmitters.

5.1 Single Satellite

We model the single-satellite setting similar to the cellular network setting with one base station and multiple users, and time varying channel conditions in [24, 25]. The main difference from the cellular network setting is that a ground station can only be served by the satellite for a small number of slots in a day. Consider all the time slots $\{1, \ldots, T\}$. We can ignore the slots in which no ground stations can be served the satellite. Let $\mathcal{T}$ denote the set of remaining slots, i.e., slots in which at least one ground station can be served by the satellite. The scheduling algorithm below only considers slots in $\mathcal{T}$.

To achieve high aggregate key rate, while maintaining certain degree of fairness among the ground stations, we use the *minimum-performance guarantee* scheduling framework in [25], which provides an absolute rate guarantee for each ground station. Specifically, let $r_g \geq 0$ denote the minimum average key rate for ground station g over $\mathcal{T}$. Let $U_g^t \geq 0$ denote the level of performance (or utility) obtained when the satellite serves ground station g in slot t. For example, U_g^t can be the number of key bits established between the satellite and the ground in slot t. Let $\vec{U}^t = \left(U_g^t, \forall g \in \mathcal{G}\right)$ represent the vector of key rate for all the ground station in slot t. For ease of exposition, we omit the superscript t and let $\vec{U} = (U_g, \forall g \in \mathcal{G})$ represent a vector of random variables, where U_g represents the performance value of ground station g in a generic time slot. A policy Q determines which ground station is served by the satellite.

The problem of optimal minimum-performance guarantee scheduling is to find a policy

$$\text{maximize}_{Q \in \Theta} \quad \mathbb{E}\left(\sum_g U_g \mathbf{1}_{Q(\vec{U})=g}\right) = \sum_g \mathbb{E}\left(U_g \mathbf{1}_{Q(\vec{U})=g}\right) \tag{14}$$

$$\text{subject to} \quad \mathbb{E}\left(U_g \mathbf{1}_{Q(\vec{U})=g}\right) \geq r_g \tag{15}$$

where Θ represents the set of all stationary policies, $\mathbf{1}_{Q(\vec{U})=g}$ is an indicator function, i.e., it is 1 if the policy selects ground station g, and 0 otherwise. In other words, an optimal policy Q^* satisfies that for each ground station g, its average key rate with the satellite is at least r_g and the the total expected system performance is maximized.

The study in [25] identifies an optimal policy as

$$Q^*(\vec{U}) = \arg\max_g[(1 + \lambda_g^*)U_g] \tag{16}$$

where the λ_g^*'s are real parameters satisfying (i) $\min_g(\lambda_g^*) = 0$; (ii) For all $g \in \mathcal{G}$, $\mathbb{E}\left(U_g \mathbf{1}_{Q^*(\vec{U})=g}\right) \geq r_g$; and (iii) For all $g \in \mathcal{G}$, if $\mathbb{E}\left(U_g \mathbf{1}_{Q^*(\vec{U})=g}\right) > r_g$, then $\lambda_g^* = 0$, .

Intuitively, the above policy selects the relatively-best ground station, i.e., ground station g that has the highest $(1 + \lambda_g^*)U_g$, where the non-negative parameters λ_g^*'s scale the performance values. This policy increases the chance that the ground stations under unfavorable conditions are selected, so that their minimum rate guarantee is achieved, i.e., satisfying $\mathbb{E}\left(U_g \mathbf{1}_{Q^*(\vec{U})=g}\right) = r_g$. For the favorable ground stations, i.e., those with $\mathbb{E}\left(U_g \mathbf{1}_{Q^*(\vec{U})=g}\right) > r_g$, they get higher rates than their pre-determined minimum rates, taking advantage their higher key rates.

The optimal policy in (16) requires estimating parameters, λ_g^*, for each ground station g. Let vector $\vec{\lambda}^* = (\lambda_g^*, \forall g \in \mathcal{G})$ represent the scalars for all the ground stations. Based on the conditions that if $\lambda_g^* > 0$, then $\mathbb{E}\left(U_g \mathbf{1}_{Q^*(\vec{U})=g}\right) = r_g$, we see that $\vec{\lambda}^*$ is a root of $f(\vec{\lambda}) = 0$; the component for

satellite g in $f(\vec{\lambda})$ is defined as

$$f_g(\vec{\lambda}) = (\lambda_g - \min_{g'}(\lambda_{g'})) \left(\mathbb{E} \left(U_g \mathbf{1}_{Q^*(\vec{U})=g} \right) - r_g \right).$$

Following the approach in [25], we use stochastic approximation to obtain the root λ_g^* through a sequence of iterates, $\lambda_g^1, \lambda_g^2, \ldots$. Each iterate λ_g^t defines a policy for slot t as

$$Q^t(\vec{U}^t) = \arg\max_g [(1 + \lambda_g^t)U_g^t]. \tag{17}$$

The update rule is

$$\lambda_g^{t+1} = \left[\lambda_g^t - \delta^t \left(U_g^t \mathbf{1}_{Q^t(\vec{U}^t)=g} - r_g \right) \right]^+ \tag{18}$$

where δ^t is a small positive step size that controls the update rate; $U_g^t \mathbf{1}_{Q^t(\vec{U}^t)=g}$ is U_g^t if policy Q^t schedules the satellite to serve g in slot t, and 0 otherwise; r_g is the pre-determined minimum performance, and $[x]^+ = \max(x, 0)$ ensures that $\lambda_g^{t+1} \geq 0$.

Practical considerations. We set the initial value, $\lambda_g^1 = 0$, $\forall g \in \mathcal{G}$. For simplicity, the update step size, δ^t, is set to a small constant, 0.01. We further normalize all the key rates, U_g^t, and the predetermined minimum key rate, r_g, by the maximum key rate of all the ground stations served by the satellite over all the slots, so that they are in $[0, 1]$. The update rule in (18) requires a long sequence of time slots to reach convergence. We repeat time slots in $\mathcal{T}$ multiple times until convergence. We then use the policy for the last intervals of $\mathcal{T}$ as the optimal opportunistic policy.

5.2 Multiple Satellites

We now consider the more general case of multiple satellites serving a set of ground stations. Let $\mathcal{T}_s$ denote the set of slots for satellite s in which at least one ground station can be served by satellite s. Let $\mathcal{T} = \bigcup_{s \in \mathcal{S}} \mathcal{T}_s$. We consider the slots in $\mathcal{T}$ for multi-satellite scheduling. Let $r_{s,g}$ denote the pre-determined minimum key rate for ground station g served by satellite s. Let $U_{s,g}^t \geq 0$ denote the key rate when satellite s serves ground station g in slot t. Let $\vec{U}_s^t = \left(U_{s,g}^t, \forall g \in \mathcal{G} \right)$ represent the vector of key rates for all the ground stations when served by satellite s in slot t.

Simply treating all the satellites independently, we define policy Q_s^t for satellite s and scalar $\lambda_{s,g}^t$ as in the single-satellite case. Then directly following (17) and (18), the policy for each satellite s in $\forall t \in \mathcal{T}_s$ is

$$Q_s^t(\vec{U}_s^t) = \arg\max_g [(1 + \lambda_{s,g}^t)U_{s,g}^t]. \tag{19}$$

The update rule is

$$\lambda_{s,g}^{t+1} = \left[\lambda_{s,g}^t - \delta^t \left(U_{s,g}^t \mathbf{1}_{Q_s^t(\vec{U}_s^t)=g} - r_{s,g} \right) \right]^+. \tag{20}$$

The above policy, however, does not account for the coupling of the satellites in multi-satellite scenarios.

Two examples are shown in Fig. 3. Let $w_{s,g}^t := (1 + \lambda_{s,g}^t)U_{s,g}^t$. We refer to $w_{s,g}^t$ as the *weight* for satellite s and ground station g in slot t, represented as a line connecting s and g; the thicker the line, the larger weight. Figures 3a and b show the actions of two satellites, s_1 and s_2, are coupled since both of them can serve ground station g_2. In Fig. 3a, following (19), satellites s_1 and s_2 serve ground stations g_1 and g_2, respectively. In Fig. 3b, however, the weight between s_1 and g_2 is the largest. If s_1 serves g_2, then g_1 will not be served in that slot. An alternative strategy schedules s_1 to serve g_1, and s_2 to serve g_2. It leads to a more balanced key rate among the ground stations, and hence more desirable for generating pairwise keys among ground station pairs in Phase 2 (see §4), even though the total key rate is lower than the of the first strategy.
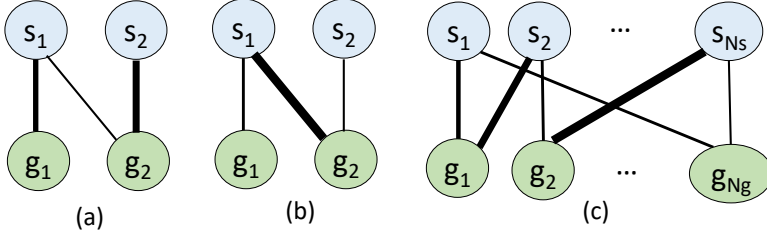
Fig. 3. Bipartite graph representing the relationship between satellites and ground stations in one time slot. A satellite is connected to a ground station if it can serve the ground station in that slot. A thicker line connecting satellite s and ground station g represents a higher weight, $w_{s,g}^t$. In (a) and (b), we show two examples that illustrate the coupling of the satellites; a general case is shown in (c).

5.2.1 Multi-satellite Scheduling. In general, we model the multi-satellite scheduling problem as a bipartite graph. In each slot, we consider the set of satellites that can serve at least one ground station, and the set of ground stations that can be served by at least one satellite. The connection between satellite s and g is marked as the weight, $w_{s,g}^t$. Scheduling the satellites can then be modeled as a bipartite matching problem.

Let N_S and N_G denote respectively the number of satellites and ground stations in the graph (we omit the superscript t for clarity). We may have $N_S < N_G$, $N_S = N_G$, or $N_S > N_G$. Since N_S may not equal N_G, some satellites may not be scheduled to serve any ground station if $N_S > N_G$, or a ground station may not be served if $N_S < N_G$. As illustrate earlier, since more balanced keys among the ground stations and satellites can lead to more balanced pairwise keys across the ground stations, we want to use all the satellites if $N_S \leq N_G$, or serve all the ground stations if $N_S \geq N_G$. We model the problem as a two-dimensional (2D) assignment problem, also known as the linear sum assignment problem [10]. In the following, we describe the problem assuming $N_G \leq N_S$; the other case can be simply modeled by switching satellite and ground stations.

Consider a $N_G \times N_S$ matrix $\mathbf{W}$ of weights, where the weights are as defined above. The 2D rectangular assignment problem consists of choosing one element in each row and at most one element in each column (i.e., using one satellite to serve a ground station) such that the sum of the chosen elements maximized. Specifically, it solves an optimization problem

$$\mathbf{X}^* = \arg\max_{\mathbf{x}} \sum_{i=1}^{N_G} \sum_{j=1}^{N_S} w_{i,j} x_{i,j} \tag{21}$$

$$\text{subject to} \quad \sum_{j=1}^{N_S} x_{i,j} = 1, \qquad\qquad \forall i = 1, \dots, N_G \tag{22}$$

$$\sum_{i=1}^{N_G} x_{i,j} \leq 1, \qquad\qquad \forall j = 1, \dots, N_S \tag{23}$$

$$x_{i,j} \in \{0, 1\}, \qquad\qquad \forall i = 1, \dots, N_G, \forall j = 1, \dots, N_S \tag{24}$$

The optimal solution $\mathbf{X}^*$ determines the schedule for the slot.

The above 2D assignment problem can be solved efficiently using polynomial algorithms. When $N_S = N_G = N$, it can be solved using the Hungarian algorithm with the complexity of $O(N^3)$ [10]. For the more general case, it can be solved using the JVC algorithm [14, 17]. We use `linear_sum_assignment` in `scipy.optimize` to solve it, which uses a modified JVC algorithm [12].

After obtaining the schedule for satellite s in slot t, we use the update rule in (20) to obtain $\lambda_{s,g}^{t+1}$ for the next slot. We again set the initial value, $\lambda_{s,g}^{1} = 0$, $\forall s, \forall g$, and set δ^t to 0.01. The key rate values $U_{s,g}^{t}$ and $r_{s,g}$ are normalized by the maximum key rate of all the ground stations and satellites over all the slots. We again repeat time slots in $\mathcal{T}$ multiple times until convergence, and take the policy in the last $\mathcal{T}$ as the schedule.

In summary, the above multi-satellite scheduling algorithm combines single-satellite scheduling and 2D assignment to determine the schedule for each satellite in each slot. Because of the 2D assignment, the schedule for a satellite does not necessarily follow (19) and it is not clear whether the minimum rate $r_{s,g}$ is guaranteed for satellite s and ground station g. In §6, we show, empirically, that the minimum rate is satisfied for the above algorithm for all the cases that we evaluate. Further analytical study is left as future work.

5.2.2 Predetermining Minimum Rates. We next design two heuristic algorithms, Round-Robin (RR) and Greedy heuristic, to determine the key rate, $r_{s,g}$, $\forall s, \forall g$, beforehand, which is used as input to our opportunistic scheduling algorithm.

• **RR.** Recall that $\mathcal{T}$ represents the set of slots in which at least one satellite can serve at least one ground station. We design RR so that each satellite serves each ground station for a similar number of slots. Specifically, we keep a counter $C_{s,g}$, which denotes the number of slots for which satellite s has served ground station g at the end of $\mathcal{T}$, $\forall s, \forall g$. All the counters are initialized to zero. We then find all the slots in $\mathcal{T}$, in which a single ground station, g, can only be served by a single satellite, s, and s is not in view of any other ground stations. For these slots, we directly schedule satellite s to serve g, and increment the counter, $C_{s,g}$, accordingly. After that, we consider the remaining slots in $\mathcal{T}$ sequentially. For each of these slots, we consider a weighted bipartite graph, where a satellite s is connected to a ground station g if s can serve g in that slot, and the weight of the edge is set to the current value of $C_{s,g}$. To prioritize the satellite and ground station pairs that have lower count, we use 2D assignment (as in §5.2.1), with the goal of minimizing the sum of the weights. The output of the 2D assignment determines which satellite serves which ground station in each slot.

• **Greedy heuristic.** We design this heuristic to prioritize key rate, with some consideration of fairness. Specifically, in each slot t, let S_g^t denote the set of satellites that can serve ground station g. This greedy heuristic chooses the satellite $s \in S_g^t$ that has the highest key rate with g to serve g. A *conflict* occurs if the same satellite is the best satellite for two ground stations, g and g', since a satellite can only serve a single ground station at one point of time (assuming each satellite has a single transmitter). In this case, the satellite s is assigned to the ground station with which s has fewer key bits so as to balance the number of key bits between s and the ground stations. This heuristic may cause a satellite s to generate many key bits with one ground station, but only a small number of key bits with other ground stations, which will limit the number of key bits that can be generated for ground station pairs through s in Phase 2.

For both of these heuristics, once the satellite schedules are determined, we can obtain the total number of key bits that satellite s generates with ground station g over $\mathcal{T}_s$, i.e., the subset of time slots in $\mathcal{T}$ in which satellite s is in view of at least one ground station. We then obtain the average key rate as the total number of key bits divided by $|\mathcal{T}_s|$, which is used as $r_{s,g}$ for multi-satellite opportunistic scheduling.

6 Performance Evaluation

6.1 Evaluation Setup

We consider a polar constellation of LEO satellites in 20 rings, each ring with 20 satellites for a total of 400 satellites as in [21, 29]. Let A denote the attitude of the satellites. We set A to 500 km,

800 km, or 1000 km. Each satellite is equipped with a photon source that operates at a one GHz rate, i.e., generating 10^9 photons per second. We consider two QKD deployment scenarios: *global* deployment with 11 ground stations in 5 continents and *regional* deployment with 4 ground stations in North America. Specifically, the 11 ground stations in 5 continents include New York City (NYC), Washington D.C. (DC), Toronto, Houston, and Boston in North America, London and Dublin in Europe, Singapore and Mumbai in Asia, Sydney in Australia, and Johannesburg in Africa. They represent an envisioned global QKD system that provides inter-continental coverage. The 4 ground stations in North America include NYC, DC, Toronto, and Houston, which is a smaller-scale QKD system that is easier to deploy. Considering the constraints of the current technologies, we focus on the setting where each satellite has a single transmitter and each ground station has a single receiver, i.e., $M_s = 1$, $R_g = 1$, $\forall s \in \mathcal{S}$ and $\forall g \in \mathcal{G}$.

We consider four days, the 15th day of March, June, September, and December, that represent different seasons of a year. Specifically, the channel models follow the actual weather and background photon measurement data for these four days in 2022, as described in §2.2. For each day, we obtain the satellite schedules for each slot of one second. Therefore, one day contains $T = 86,400$ slots. The elevation angle threshold is set to $\theta = 20°$, i.e., a satellite can only serve a ground station when the elevation angle to the ground station is larger than $20°$.

Performance metrics. We evaluate the various scheduling strategies using two performance metrics: (i) *minimum key size*, i.e., the minimum number of secret key bits that are generated for the ground station pairs at the end of a day, and (ii) *total key size*, i.e., the sum of the secret key bits generated for all ground station pairs at the end of a day. The first metric represents fairness among the ground station pairs, while the second one represents overall system throughput. A desirable scheduling algorithm achieves an effective balance between these two metrics.

Comparison schemes. We evaluate two opportunistic scheduling schemes, *Op-RR* and *Op-Greedy*. They use respectively the outputs of the two heuristic schemes, *Round-Robin (RR)*, and *Greedy heuristic*, as input to opportunistic scheduling in Phase 1, and then the iterative optimization in (11) for Phase 2. We compare them with the results when using RR and Greedy for Phase 1 directly (i.e., without opportunistic scheduling) and then the same iterative optimization approach for Phase 2. In addition, we compare them with the results from the *Max-Min* formulation, which is optimal in terms of the minimum key size metric, and the *Max-Sum* formulation, which is optimal in terms of the total key size metric, see §3.2. Both Max-Min and Max-Sum rely on solving large-scale MIP problems. We obtain results for these problems using CPLEX [1] running on a high-performance computing facility with over 300 GB memory, and each problem instance takes multiple hours to complete. The two opportunistic scheduling schemes are much more scalable, taking only minutes to run, with little memory requirement.

6.2 Need for Satellite Scheduling

For both the global and regional QKD settings, a satellite can be in view of multiple ground stations, and a ground station can be in view of multiple satellites in a slot, hence presenting the need for scheduling satellites. Fig. 4 shows the distribution plots for the global QKD setting for the day in September; the results the other three days are similar. The top row shows the histogram of the number of ground stations that a satellite can choose to serve in a slot, considering all the satellites and slots. The results for $A = 500$, 800, and 1000 km are shown in the figure. We see a significant number of instances when a satellite can choose from multiple ground stations to serve in a slot, and the number of choices increases with altitude. Specifically, the maximum number of ground stations that a satellite can choose from is 4 when $A = 500$ km, and 5 when $A = 800$ and 1000 km. The bottom row of Fig. 4 shows the histogram of the number of satellites that can serve a ground station in a slot, considering all the ground stations and slots in a day. Only when $A = 500$ km, a

(a) $A = 500$ km, satellite view. (b) $A = 800$ km, satellite view. (c) $A = 1000$ km, satellite view.

(d) $A = 500$ km, GS view. (e) $A = 800$ km, GS view. (f) $A = 1000$ km, GS view.
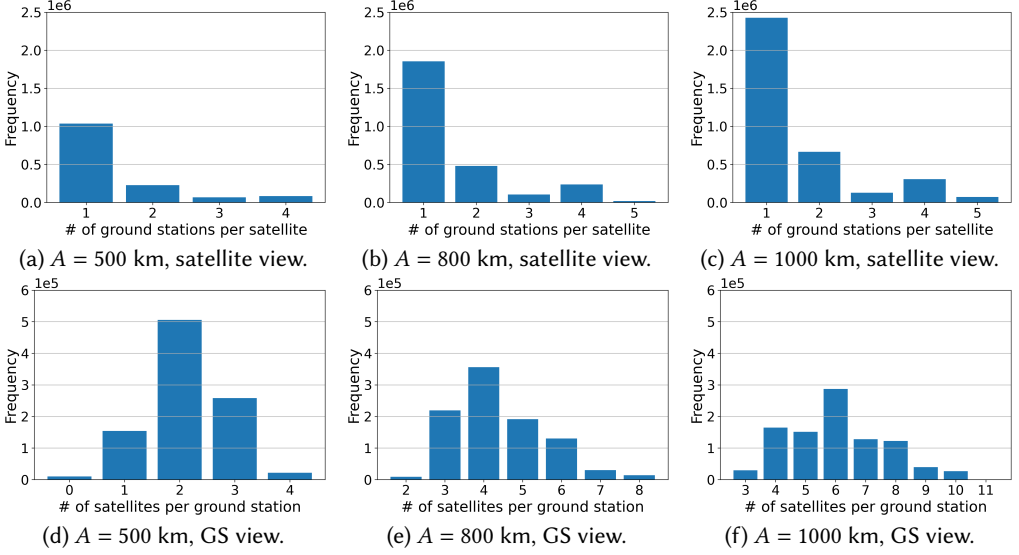
Fig. 4. Global QKD setting. Top row: satellite view, i.e., histogram of the number of ground stations that can be served by a satellite in a slot. Bottom row: ground station (GS) view, i.e., histogram of the number of satellites that can serve a ground station in a slot. Both rows consider all the slots for the day in September.

ground station is sometimes not in view of any satellite in one slot (and hence cannot be served in that slot); for $A = 800$ km, a ground station can be served by 2 to 8 satellites, which is increased to 3 to 11 satellites when $A = 1000$ km. The above results demonstrates the need for satellite scheduling. The regional QKD setting exhibits similar trends as in Fig. 4, with slightly less ground stations (up to 4) that a satellite can choose to serve, and less satellites (up to 9) that can serve a ground station in a slot.

We next briefly describe the statistics regarding Phase 1 opportunistic scheduling. Recall that $\mathcal{T}_s$ represents the slots that satellite s are considered in the scheduling. For the global QKD setting, the average $|\mathcal{T}_s|$ values are 3537, 6734, and 8999 when $A = 500$, 800, and 1000 km, respectively. For the regional QKD setting, the values are lower, as 1130, 1952, and 2487. In each slot, opportunistic scheduling considers a bipartite graph connecting a subset of satellites and ground stations, with an edge connecting a satellite and ground station if that satellite can serve the ground station. For the global QKD setting, when $A = 500$ km, the number of ground stations in a slot varies from 9 to 11 (i.e., most or all of the ground stations can be served by at least one satellite), and the number of satellites is larger, varying from 11 to 21; for $A = 800$ and 1000 km, the number of ground stations is 11 per slot, and the number of satellites varied from 24 to 38, and 35 to 49, respectively. For the regional QKD setting, when $A = 500$ km, the number of ground stations in a slot varies from 3 to 4 (i.e., most or all of the ground stations can be served by at least one satellite), and the number of satellites varies from 2 to 8; for $A = 800$ and 1000 km, the number of ground stations is 4 per slot, and the number of satellites varies from 6 to 12, and 9 to 14, respectively.

6.3 Results for Global QKD Setting

We now present the results for the global QKD setting with 11 ground stations in 5 continents. We first present the results assuming no cloud coverage, i.e., $c_{t,g} = 0$, $\forall t$, $\forall g \in \mathcal{G}$, in §6.3.1. This is an idealistic setting that provides the best performance. It serves as an upper bound of realistic settings that have cloud coverage, which we present next in §6.3.2.

(a) Op-RR versus RR.
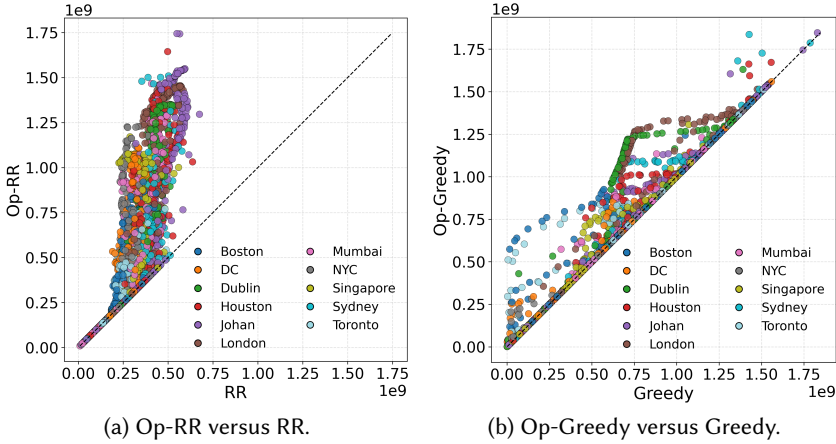
(b) Op-Greedy versus Greedy.

Fig. 5. Key size (in bits) obtained for each satellite and ground station pair at the end of one day (i.e., Phase 1 results), global QKD setting, $A = 500$km, for the day in September.
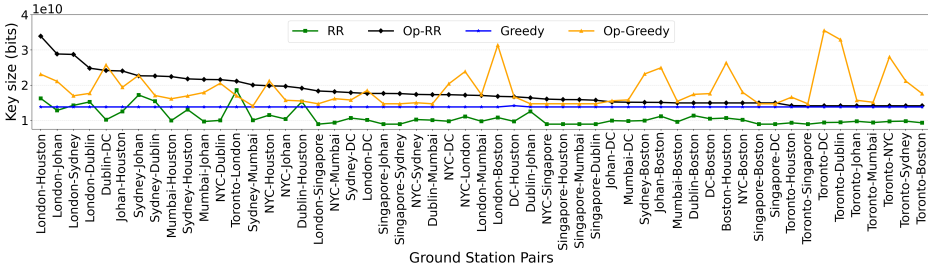

Fig. 6. Key size (bits) for each of the 55 ground station pairs in the global QKD setting for Op-RR and Op-Greedy versus RR and Greedy, $A = 500$ km, for the day in September, assuming no cloud coverage.

6.3.1 No Cloud Coverage. We first show the results for the two opportunistic schemes, Op-RR and Op-Greedy, during Phase 1. Specifically, these two schemes take respectively the key rate from RR and Greedy as input, and opportunistically schedule the satellites to serve the ground stations. Fig. 5a shows a scatter plot of the total number of key bits generated for each satellite and ground station pair over one day using Op-RR versus that obtained by RR, when $A = 500$km and for the September day (the results for the other three days are similar). We see that the number of key bits obtained by Op-RR is significantly larger than the corresponding value under RR for most cases, except for those cases where these two schemes obtain the same results. Fig. 5b compares the total number of key bits obtained for each satellite and ground station pair using Op-Greedy versus that obtained by Greedy. We again see that the opportunistic strategy leads to more or equal key bits for each satellite and ground station pair. Comparing Fig. 5a and b, we see that the RR leads a much narrower range of values compared to the Greedy heuristic, which is consistent with the design goal of RR that aims to obtain similar number of key bits for satellite and ground station pairs.

Fig. 6 shows the key size (in bits) for each of the 55 ground station pairs for four schemes, RR, Greedy, Op-RR and Op-Greedy, sorted in descending order according to Op-RR. As expected, since Op-RR obtains more key bits per satellite and ground station pair than RR in Phase 1, the number of key bits per ground station pair under Op-RR is higher than that under RR. Similar argument holds for Op-Greedy versus Greedy. We see that the number of key bits per ground station pair is similar across the ground station pairs under the Greedy heuristic, which is not necessarily true

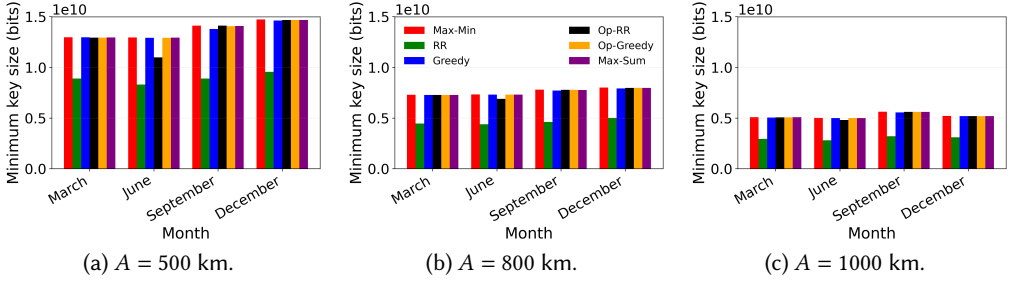(a) $A = 500$ km.   (b) $A = 800$ km.   (c) $A = 1000$ km.

Fig. 7. Minimum key size (bits) across the 55 ground station pairs in the global QKD setting, assuming no cloud coverage.

in other scenarios, a point that we will return to later on. Last, while both Op-RR and Op-Greedy lead to more key bits than RR and Greedy, they lead to different distribution of key bits across the ground station pairs.

Fig. 7 shows the minimum key size (in bits) across all the ground station pairs. The results for Max-Min, RR, Greedy, Op-RR, Op-Greedy, and Max-Sum are shown in the figure. Max-Min leads to the optimal results for this setting. In contrast, Max-Sum favors the cases with high key rate, which can lead to unfair key rates to some ground station pairs. Interestingly, for this setting, we see Max-Sum leads to similar results as Max-Min in all the scenarios. This is perhaps due to the averaging effect when considering a large number of ground station pairs, a point that we will return to in §6.4 for the regional QKD setting. RR leads to the lowest minimum key size in all the scenarios. Op-RR, on the other hand, leads to values close to the optimal value in most cases, except for the day in June and $A = 500$ km. Greedy and Op-Greedy lead to results close to the optimal values in all the settings, which is not always true, as we shall see later when considering realistic settings with cloud coverage.

In Fig. 7, we see higher minimum key size for the two days in September and December than the other two days, which is particularly noticeable for $A = 500$ km. This is due to better weather conditions for most ground stations in these two days. For the same day, we see lower minimum key size when increasing the satellite altitude. This is because, even though higher altitudes lead to better coverage, the transmissivity of the channel from a satellite to a ground station degrades with distance.

Fig. 8 plots the total key size (in bits) across the 55 ground station pairs, where Max-Sum leads to the optimal result in each scenario. The two opportunistic schemes lead to results closest to the optimal solutions in all the scenarios, significantly outperform their heuristic counterparts, and the results from Max-Min. Specifically, the value of Op-RR is 72% to 73% of the corresponding optimal values, while for Op-Greedy, the range is 75% to 76%. For each altitude, the results for the four seasons are similar. We see lower total key size when increasing the satellite altitude due to lower transmissivity.

6.3.2 Considering Cloud Coverage. We now present the results when considering cloud coverage. For each day, for convenience, we obtain the cloud coverage at the beginning of each hour (see §2.2) and use it as the cloud coverage for each slot in that hour. Fig. 9 plots the average cloud coverage for each ground station for the four days in March, June, September, and December, sorted in descending order according to the cloud coverage in March; the standard deviation is large for many cases and is omitted in the plot for clarity. For each day, we see significantly different cloud coverage across the ground stations. For the same ground station, the cloud coverage can also differ substantially since the four days correspond to different seasons. For the day in June, all the ground
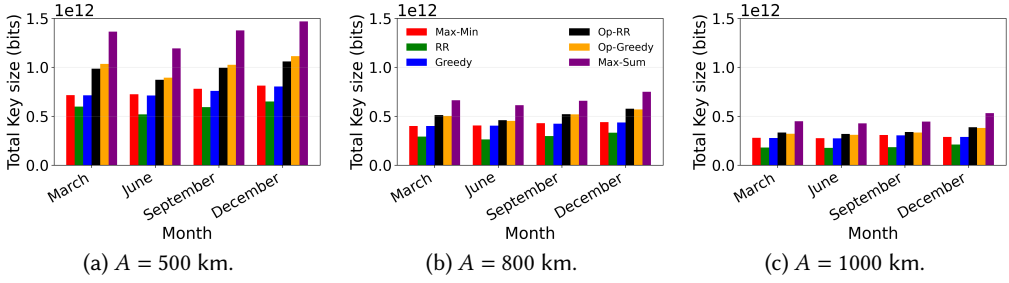
Fig. 8. Total key size (bits) over the 55 ground station pairs in the global QKD setting, assuming no cloud coverage.
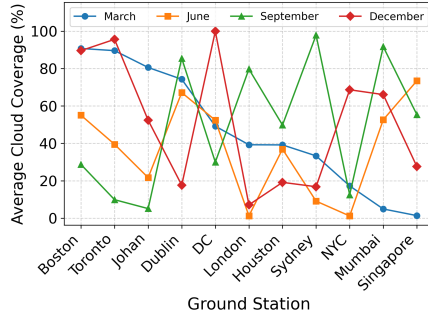

Fig. 9. Average cloud coverage over a day for the 11 ground stations; standard deviation omitted for clarity.

stations have generally low cloud coverage, while DC has the highest average cloud coverage in the day in December, followed by Sydney for the day in September.

Since some ground stations have high cloud coverage in some slots, which leads to low key rate, including them in the scheduling problem can lead to inefficient usage of the resources. We therefore consider a *filtering* approach, which ignores a ground station in the scheduling problem in a slot if its cloud coverage in that slot is above a threshold. In the rest of the paper, we use a threshold of 0.8. When using the above filtering approach, if a ground station has cloud coverage above the threshold for an entire day, it will not obtain any key with any other ground stations. For the days in March and December, one ground station (Boston and DC, respectively) ends up having no keys with others. For the day in September, two ground stations (Sydney and Mumbai) have no keys with others. For the day in June, all ground stations have positive key rate with others.

The top and bottom plots in Fig. 10 show respectively the minimum and total key size across the ground station pairs for $A = 500$km; the results for the other two altitudes show similar trends and are omitted. In the figure, the solid color bars represent the results when not applying filtering, while the bars with slashed lines represent the results when applying filtering. We use log scale for these two plots since the values in each plot can differ in orders of magnitude.

We first present the results when not applying filtering (i.e., the solid color bars). As expected, due to cloud coverage, both minimum and total key sizes are significantly lower than those without cloud coverage (see Fig. 7a and Fig. 8a). Specifically, for minimum key size, the largest value is 3.4×10^9 bits (Max-Min for the day in June), only 23% of the largest value without cloud coverage. For total key size, the largest value is 8.5×10^{11} bits (Max-Sum for the day in June), only 58% of the largest value without cloud coverage. The number of key bits for the day in June is larger than those for the other days since the cloud coverage for that day is low for all ground stations. For minimum key size, we again see that the two opportunistic schemes and Max-Sum lead to results close to the optimal value (obtained by Max-Min) for all four days. For total key size, the two opportunistic
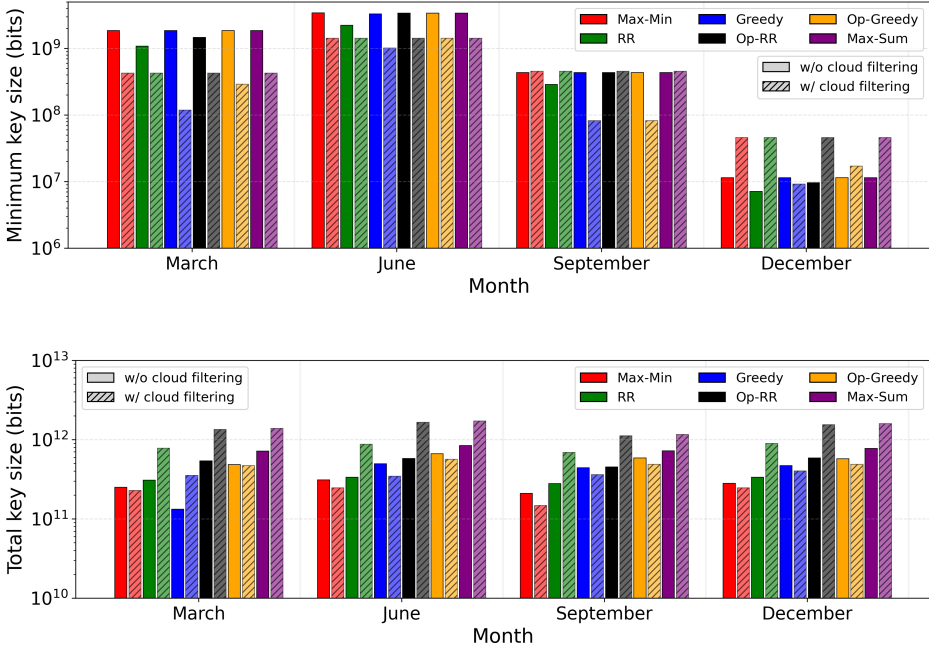
Fig. 10. Minimum (top) and total (bottom) key sizes of the ground station pairs, global QKD setting, $A = 500$ km, considering cloud coverage. The results with and without filtering are represented as solid color bars and bars with slashed lines. Key size can be zero for some ground station pairs due to filtering, which is excluded in obtaining the minimum key size in the top plot. Note the different y-axis values in the two plots.

schemes are closer to the optimal values (obtained by Max-Sum) than other schemes. Specifically, the total key size obtained by Op-RR is 63%-76% of the optimal value for the four days, while the range is 68%-82% for Op-Greedy.

We next present the results when applying filtering (i.e., the bars with slashed lines). For minimum key size, the ground stations pairs with zero key are excluded from the plot (since all schemes have minimum key size as zero in that case). Op-RR is close to the optimal value (by Max-Min) for all the four days, while Op-Greedy is only close to the optimal value for one day (in June); for the other three days, its value is only 18%, 37%, and 68% of the optimal value. For total key size, Op-RR again leads to results close to the optimal values (by Max-Min), while Op-Greedy leads to results only 31% to 42% of the optimal values. Therefore, Op-RR, which starts with a fairer key allocation by RR than Greedy, tends to lead to better results than Op-Greedy. Indeed, Greedy allocates satellites in a greedy manner in Phase 1, which may cause a satellite to have unbalanced number of key bits with ground stations, and hence does not help ground station pairs to generate keys through this satellite in Phase 2. Op-Greedy, based on Greedy, may have the same limitation.

We now compare the results when applying filtering with those when not applying filtering (i.e., comparing two adjacent bars, one solid color and the other with slashed lines in Fig. 10). For minimum key size, we only compare the results for the day in June since for all the other three days, the key rate for some ground station becomes zero due to filtering. We see for all the schemes, using filtering leads to lower minimum key size. This is as expected since the ground stations with high cloud coverage are only served in the slots with cloud coverage lower than the threshold, which can further limit their key sizes and lower the minimum key size. For total key size, filtering leads to different impacts for different schemes. We next describe its impacts on Op-RR, which is
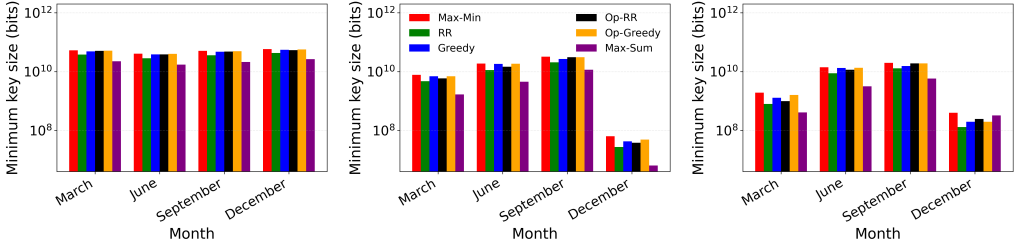
(a) Assuming no cloud coverage.   (b) W/ cloud coverage, no filtering. (c) W/ cloud coverage, w/ filtering.

Fig. 11. Minimum key size (bits) for the regional QKD setting, $A = 500$ km. In plot (c), DC has zero key with any other ground station due to filtering in December, and is excluded from the plot.
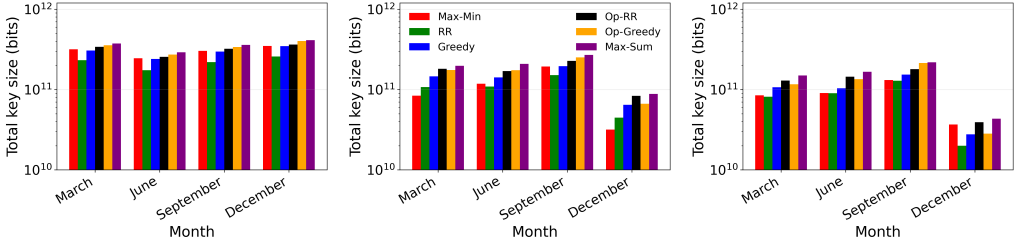
(a) Assuming no cloud coverage.   (b) W/ cloud coverage, no filtering. (c) W/ cloud coverage, w/ filtering.

Fig. 12. Total key size (bits) for the regional QKD setting, $A = 500$ km.

efficient and provides the best tradeoff of all the schemes. When using filtering, the total key size under Op-RR is 2.5-2.9× of that without filtering, demonstrating the benefits of using filtering in improving system throughput.

6.4   Results for Regional QKD Setting

For the regional QKD setting (i.e., 4 ground stations in North America), we again consider three scenarios: assuming no cloud coverage, considering cloud coverage without and with filtering. When using filtering, DC is not served for the day in December since its cloud coverage is above the threshold for all the slots.

Fig. 11 shows the minimum key size when $A = 500$ km for the three scenarios; the results for $A = 800$ and 1000 km show similar trends and are omitted. The two opportunistic schemes lead to close to optimal values (obtained using Max-Min), similar to the observation for the global QKD setting. Max-Sum leads to significantly worse performance in most cases. For instance, it leads to minimum key size only 42%-49% of the optimal values when assuming no cloud coverage. This is in contrast to the observations in the global QKD setting, where Max-Sum leads to close to optimal results. This difference is perhaps due to the small number of ground stations in the regional QKD setting, which lacks the natural averaging effect when there are a large number of ground stations at geographically distributed locations. As the global setting, we see that using filtering reduces minimum key size compared to not using filtering (see Figures 11b and c, excluding the day in December since DC has no key for that day due to filtering).

Fig. 12 shows the total key size (in bits) for the three scenarios when $A = 500$ km. We see that the results under Op-RR is close to the optimal solution (obtained using Max-Sum): it is 88%-91%, 82%-95% and 82%-91% of the optimal values for the three settings in Figures 12a to c. The gap between Op-RR and Max-Sum is even smaller in this setting than that in the global QKD setting. Op-Greedy leads to results close to the optimal solution, except for the December day in Fig. 12c, where its minimum key size is 65% of the optimal value. Unlike the global QKD setting, we see that

applying filtering reduces the total key size for Max-Sum, Op-RR and Op-Greedy for all of the four days (see Figures 12b and c). This might be due to the small number of ground stations in a small geographic region, where the resource is abundant, and hence not serving one ground station does not lead to much benefits to other ground stations.

7 Related Work

In classical wireless networks, opportunistic scheduling refers to a class of popular scheduling policies that dynamically allocates resources to users with favorable channel conditions to improve overall resource utilization [5]. Most opportunistic scheduling frameworks [4, 20, 23, 27, 36] focus on maximizing network capacity, often neglecting fairness, which can disadvantage users with persistently weak channels. To address this, several studies such as [24, 25], introduce fairness-aware scheduling policies with minimum-performance guarantees (MPG). In our work, we adapt the opportunistic scheduling principle to satellite-assisted QKD systems, building on the minimum-performance guarantee concept but extending it to a multi-satellite, multi-ground-station setting with visibility and hardware constraints, conditions not captured in classical MPG formulations.

Our scheduling problem differs fundamentally from the well-studied classical data transfer scheduling problem of satellite networks [15, 18, 35, 41], where satellites offload classical data to ground stations. They treat this problem using traditional resource allocation techniques such as Multiprocessor Scheduling, Resource-Constrained Project Scheduling, Genetic Algorithms, MIP programming. Those models involve only classical bits and do not account for the quantum or classical stages of QKD or the generation of shared secret keys among ground station pairs.

The scheduling problem for dual-downlink entanglement distribution [11, 28, 39, 40] and entanglement-based QKD [26] in satellite-based quantum networks has been studied in prior work. However, these studies primarily focus on maintaining simultaneous connectivity between a ground-station pair and a satellite, and do not account for the opportunistic selection step that arises in the single-downlink scenario, where even a single ground station can be served at any point of time. The authors in [32] consider single-downlink satellite QKD scheduling. They present an MIP formulation to schedule a single satellite to a set of ground stations with the goal of maximizing the sum of the key rates from the satellite to the ground stations. Our formulation differs significantly from that of [32], since we consider generating key bits for ground station pairs assisted by multiple satellites, taking account of both total key bits and fairness. We present MIP formulations as comparison baselines, and opportunistic scheduling approaches. In addition, our evaluation considers both global and regional QKD settings, while the work in [32] focuses on a setting with ground stations all in the UK.

8 Conclusion

In this paper, we have developed an opportunistic scheduling framework for satellite-assisted QKD systems in single-downlink settings. This framework takes advantage of the dynamic, and diverse, satellite to ground station channels, for efficient key establishment among ground station pairs assisted by the satellites. Under this framework, we developed two opportunistic scheduling schemes, Op-RR and Op-Greedy. Using extensive simulation in a wide range of settings, we show that Op-RR achieves the best tradeoffs in fairness and total key size across all the schemes that we evaluate. We further show the impact of seasonal effects, cloud coverage, and the settings of the ground stations on the key establishment results, highlighting the importance of considering these realistic factors in evaluating satellite-assisted QKD systems.

References

[1] CPLEX. https://www.ibm.com/products/ilog-cplex-optimization-studio.

[2] MODTRAN®. http://modtran.spectral.com/.

[3] Visual Crossing: Weather Data & API, Global Forecast & History Data. https://www.visualcrossing.com/weather-data.

[4] Matthew Andrews and Lisa Zhang. Scheduling algorithms for multi-carrier wireless data systems. In *Proceedings of the 13th annual ACM international conference on Mobile computing and networking*, pages 3–14, 2007.

[5] Arash Asadi and Vincenzo Mancuso. A survey on opportunistic scheduling in wireless communications. *IEEE Communications Surveys & Tutorials*, 15(4):1671–1689, 2013.

[6] M. Aspelmeyer, T. Jennewein, M. Pfennigbauer, W. R. Leeb, and A. Zeilinger. Long-distance quantum communication with entangled photons using satellites. *IEEE J. Selected Top. Quant. Electron.*, 9:1541–1551, 2003.

[7] Minu Bae, Nitish K. Panigrahy, Prajit Dhara, Md Zakir Hossain, Walter O. Krawec, Alexander Russell, Don Towsley, and Bing Wang. Blockwise post-processing in satellite-based quantum key distribution. *IEEE Network*, 2025.

[8] R. Bedington, J. M. Arrazola, and A. Ling. Progress in satellite quantum key distribution. *npj Quant. Inf.*, 3(30), 2017.

[9] C. H. Bennett and G. Brassard. Quantum cryptography: Public key distribution and coin tossing. *Theoretical Computer Science*, 560:7–11, December 2014.

[10] Rainer Burkard, Mauro Dell'Amico, and Silvano Martello. *Assignment Problems*. Society for Industrial and Applied Mathematics, Philadelphia, PA, 2009.

[11] Alena Chang, Yinxin Wan, Guoliang Xue, and Arunabha Sen. Entanglement distribution in satellite-based dynamic quantum networks. *IEEE Network*, 38(1):79–86, 2023.

[12] David F. Crouse. On implementing 2d rectangular assignment algorithms. *IEEE Transactions on Aerospace and Electronic Systems*, 52(4):1679–1696, August 2016.

[13] Daniele Dequal, Luis Trigo Vidarte, Victor Roman Rodriguez, Giuseppe Vallone, Paolo Villoresi, Anthony Leverrier, and Eleni Diamanti. Feasibility of satellite-to-ground continuous-variable quantum key distribution. *npj Quantum Information*, 7(1):3, 2021.

[14] Oliver Drummond, David A. Castañon, and Martin Bellovin. Comparison of 2-D assignment algorithms for sparse, rectangular, floating point, cost matrices. *Journal of the SDI Panels on Tracking*, 4:81–97, 1990.

[15] C Han, X Wang, G Song, and R Leus. Scheduling multiple agile earth observation satellites with multiple observations. *arXiv:1812.00203*, 2018.

[16] T. Jennewein and B. Higgins. The quantum space race. *Phys. World*, 26(52), 2013.

[17] Roy Jonker and Anton Volgenant. A shortest augmenting path algorithm for dense and sparse linear assignment problems. *Computing*, 38(4):325–340, March 1987.

[18] D Karapetyan, SM Minic, KT Malladi, and AP Punnen. Satellite downlink scheduling problem: a case study. *Omega*, 53:115–23, 2015.

[19] Jonathan Katz and Yehuda Lindell. *Introduction to modern cryptography: principles and protocols*. Chapman and hall/CRC, 2007.

[20] Karim Khalil, Mehmet Karaca, Ozgur Ercetin, and Eylem Ekici. Optimal scheduling in cooperate-to-join cognitive radio networks. In *2011 Proceedings IEEE INFOCOM*, pages 3002–3010. IEEE, 2011.

[21] S. Khatri, A. J. Brady, R. A. Desporte, M. P. Bart, and J. P. Dowling. Spooky action at a global distance: analysis of space-based entanglement distribution for the quantum internet. *npj Quantum Inf*, 7(4), 2021.

[22] Sheng-Kai Liao, Wen-Qi Cai, Wei-Yue Liu, Liang Zhang, Yang Li, Ji-Gang Ren, Juan Yin, Qi Shen, Yuan Cao, Zheng-Ping Li, et al. Satellite-to-ground quantum key distribution. *Nature*, 549(7670):43–47, 2017.

[23] Shihuan Liu, Lei Ying, and R Srikant. Scheduling in multichannel wireless networks with flow-level dynamics. In *Proceedings of the ACM SIGMETRICS international conference on Measurement and modeling of computer systems*, pages 191–202, 2010.

[24] X. Liu, E. Chong, and N. Shroff. Opportunistic transmission scheduling with resource-sharing constraints in wireless networks. *IEEE Journal on Selected Areas in Communications*, 19(10), 2001.

[25] Xin Liu, Edwin K. P. Chong, and Ness B. Shroff. A framework for opportunistic scheduling in wireless networks. *Computer Networks*, 41(4):451–474, 2003.

[26] Ronald Maule, Nitish K. Panigrahy, Naga Lakshmi Anipeddi, Prajit Dhara, Deirdre Kilbane, Md. Zakir Hossain, Walter O. Krawec, Don Towsley, and Bing Wang. Fair and efficient scheduling strategies for satellite assisted quantum key distribution systems. *Proc. of QCE*, 2024.

[27] Michael J Neely, Eytan Modiano, and Charles E Rohrs. Dynamic power allocation and routing for time varying wireless networks. In *IEEE INFOCOM 2003. Twenty-second Annual Joint Conference of the IEEE Computer and Communications Societies (IEEE Cat. No. 03CH37428)*, volume 1, pages 745–755. IEEE, 2003.

[28] Nitish K Panigrahy, Prajit Dhara, Don Towsley, Saikat Guha, and Leandros Tassiulas. Optimal entanglement distribution using satellite based quantum networks. In *IEEE INFOCOM Workshops*, 2022.

[29] Nitish K. Panigrahy, Prajit Dhara, Don Towsley, Saikat Guha, and Leandros Tassiulas. Optimal entanglement distribution using satellite based quantum networks. In *NetSciQCom: Network Science for Quantum Communication Networks, in conjunction with Infocom*, May 2022.

[30] Stefano Pirandola, Ulrik L Andersen, Leonardo Banchi, Mario Berta, Darius Bunandar, Roger Colbeck, Dirk Englund, Tobias Gehring, Cosmo Lupo, Carlo Ottaviani, et al. Advances in quantum cryptography. *arXiv preprint arXiv:1906.01645*, 2019.

[31] Stefano Pirandola, Ulrik L Andersen, Leonardo Banchi, Mario Berta, Darius Bunandar, Roger Colbeck, Dirk Englund, Tobias Gehring, Cosmo Lupo, Carlo Ottaviani, et al. Advances in quantum cryptography. *Advances in optics and photonics*, 12(4):1012–1236, 2020.

[32] Mateusz Polnik, Luca Mazzarella, Marilena Di Carlo, Daniel KL Oi, Annalisa Riccardi, and Ashwin Arulselvan. Scheduling of space to ground quantum key distribution. *EPJ Quantum Technology*, 7(3), 2020.

[33] Renato Renner. Security of quantum key distribution. *International Journal of Quantum Information*, 6(01):1–127, 2008.

[34] C. Simon. Towards a global quantum network. *Nat. Photonics*, 11:678–680, 2017.

[35] S Spangelo, J Cutler, K Gilson, and A Cohn. Optimization-based scheduling for the single-satellite, multi-ground station communication problem. *Comput Oper Res.*, 57:1–16, 2015.

[36] Leandros Tassiulas. Scheduling and performance limits of networks with constantly changing topology. *IEEE transactions on information theory*, 43(3):1067–1073, 2002.

[37] Giuseppe Vallone, Davide Bacco, Daniele Dequal, Simone Gaiarin, Vincenza Luceri, Giuseppe Bianco, and Paolo Villoresi. Experimental satellite quantum communications. *Physical Review Letters*, 115(4):040502, 2015.

[38] Jian-Yu Wang, Bin Yang, Sheng-Kai Liao, Liang Zhang, Qi Shen, Xiao-Fang Hu, Jin-Cai Wu, Shi-Ji Yang, Hao Jiang, Yan-Lin Tang, et al. Direct and full-scale experimental verifications towards ground–satellite quantum key distribution. *Nature Photonics*, 7(5):387–393, 2013.

[39] Xinliang Wei, Lei Fan, Yuanxiong Guo, Zhu Han, and Yu Wang. Optimizing satellite-based entanglement distribution in quantum networks via quantum-assisted approaches. In *2024 International Conference on Quantum Communications, Networking, and Computing (QCNC)*, pages 280–287. IEEE, 2024.

[40] Albert Williams, Nitish K Panigrahy, Andrew McGregor, and Don Towsley. Scalable scheduling policies for quantum satellite networks. In *2024 IEEE International Conference on Quantum Computing and Engineering (QCE)*, volume 1, pages 1760–1769. IEEE, 2024.

[41] F Xhafa, J Sun, A Barolli, A Biberaj, and L Barolli. Genetic algorithms for satellite scheduling problems. *Mob Inf Syst*, 8(4):351–77, 2012.

[42] Juan Yin, Yuan Cao, Shu-Bin Liu, Ge-Sheng Pan, Jin-Hong Wang, Tao Yang, Zhong-Ping Zhang, Fu-Min Yang, Yu-Ao Chen, Cheng-Zhi Peng, et al. Experimental quasi-single-photon transmission from satellite to earth. *Optics express*, 21(17):20032–20040, 2013.